Draft version February 5, 2008
Preprint typeset using LaTeX style emulateapj v. 6/22/04

QUASI-PERIODIC OSCILLATIONS FROM MAGNETOROTATIONAL TURBULENCE

Phil Arras[1], Omer Blaes[2], Neal J. Turner[3]

Draft version February 5, 2008

ABSTRACT

Quasi-periodic oscillations (QPOs) in the X-ray lightcurves of accreting neutron star and black hole binaries have been widely interpreted as being due to standing wave modes in accretion disks. These disks are thought to be highly turbulent due to the magnetorotational instability (MRI). We study wave excitation by MRI turbulence in the shearing box geometry. We demonstrate that axisymmetric sound waves and radial epicyclic motions driven by MRI turbulence give rise to narrow, distinct peaks in the temporal power spectrum. Inertial waves, on the other hand, do not give rise to distinct peaks which rise significantly above the continuum noise spectrum set by MRI turbulence, even when the fluid motions are projected onto the eigenfunctions of the modes. This is a serious problem for QPO models based on inertial waves.

Subject headings: accretion, accretion disks — MHD — turbulence — waves — X-rays: binaries

1. INTRODUCTION

Millisecond variability has been observed for some time with the Rossi X-Ray Timing Explorer in both neutron star and black hole binaries (e.g. McClintock & Remillard 2004, van der Klis 2004). In addition to a broad continuum in the power spectrum, QPOs are observed. These QPOs have been modeled as hydrodynamic waves in geometrically thin accretion disks (for reviews see e.g. Wagoner 1999 and Kato 2001), or "torus-like" flows with significant radial pressure gradients (Giannios & Spruit 2004; Rezzolla et al. 2003; Kluźniak et al. 2004; Lee et al. 2004; Blaes et.al. 2006).

Turbulence seeded by the magnetorotational instability (MRI; Balbus & Hawley 1991) is widely believed to provide the stresses responsible for angular momentum transport and accretion. This raises a series of questions. Do waves idealized as hydrodynamic perturbations on a laminar background still exist in turbulent, magnetized accretion flows? Does the time-averaged flow act as a resonant cavity supporting standing waves? What is the steady-state wave amplitude due to turbulent excitation? The simplest and most controlled geometry to explore these questions is that of the shearing box (e.g. Hawley et al. 1995). One published attempt has been made to look for discrete mode frequencies in a shearing box MRI simulation (Brandenburg 2005), with negative results (see figure 7 of that paper). Analytic estimates for turbulent excitation of waves in accretion disks have been reported in Nowak & Wagoner (1993, 1995).

We revisit this problem, finding that MRI turbulence does indeed excite distinct peaks in the power spectrum, and that these peaks can be identified with certain classes of hydrodynamic modes, specifically axisymmetric acoustic waves and a global axisymmetric epicyclic oscillation. Hydrodynamic inertial wave modes, however, are *not* clearly detected, a serious problem for QPO models that are based on these modes ("g-modes" in diskoseismology parlance).

The plan of the paper is as follows. In section 2 we review the shearing box and compute the linear wave frequencies. We present power spectra from numerical simulations in section 3, and discuss the results. We present our conclusions and discuss their relevance to models for QPOs in section 4.

2. THE SHEARING BOX

We solve the magnetohydrodynamic (MHD) equations as applied to an isothermal, differentially rotating, magnetized accretion disk, in the unstratified shearing box approximation:

$$\frac{\partial \boldsymbol{v}}{\partial t} + \boldsymbol{v}\cdot\boldsymbol{\nabla}\boldsymbol{v} + 2\boldsymbol{\Omega}\times\boldsymbol{v} = -\frac{1}{\rho}\boldsymbol{\nabla}\left(P + \frac{B^2}{8\pi}\right) \quad (1)$$

$$+ \frac{\boldsymbol{B}\cdot\boldsymbol{\nabla}\boldsymbol{B}}{4\pi\rho} + 2q\Omega^2 x\boldsymbol{e}_x \quad (2)$$

$$\frac{\partial \rho}{\partial t} + \boldsymbol{\nabla}\cdot(\rho\boldsymbol{v}) = 0 \quad (3)$$

$$\frac{\partial \boldsymbol{B}}{\partial t} = \boldsymbol{\nabla}\times(\boldsymbol{v}\times\boldsymbol{B}) \quad (4)$$

$$P = c_s^2\rho. \quad (5)$$

Here ρ, P, $\boldsymbol{v}$, and $\boldsymbol{B}$ are the mass density, gas pressure, velocity and magnetic field. The sound speed c_s is constant. The simulation domain represents a small region of the disk near the midplane orbiting with frequency Ω. The non-inertial reference frame of the orbit is taken into account by including a Coriolis force, as well as "tidal" forces due to the difference of gravitational and centrifugal forces, represented by the term $2q\Omega^2 x\boldsymbol{e}_x$, where $q = -d\ln\Omega/d\ln R$ is the shear parameter. Cartesian coordinates are used, with the radial, azimuthal, and vertical coordinates labeled x, y, z, respectively. The azimuthal and vertical boundaries are periodic, and the radial boundaries are shearing-periodic (fluid passing through one radial boundary appears on the other at an azimuth that varies in time according to the difference in orbital speed across the box).

An initially weak magnetic field will drive turbulence in the shearing box due to the MRI, which is a nearly incom-

[1] Kavli Institute for Theoretical Physics, Kohn Hall, University of California, Santa Barbara, CA 93106; arras@kitp.ucsb.edu
[2] Department of Physics, Broida Hall, University of California, Santa Barbara, CA 93106; blaes@physics.ucsb.edu
[3] Jet Propulsion Laboratory, MS 169-506, California Institute of Technology, Pasadena, CA 91109; neal.turner@nasa.jpl.gov

pressible instability. A second branch of nearly incompressible perturbations which we call "inertial waves" also exists, at least on a laminar background flow. In the limit of zero magnetic field, the specific angular momentum gradient is the restoring force for these inertial waves. To understand the two solutions with a simple example, linearize about a time-independent background with constant density ρ and pressure P, constant magnetic field $\boldsymbol{B} = B_y \boldsymbol{e}_y + B_z \boldsymbol{e}_z$, and velocity $\boldsymbol{v} = -q\Omega x \boldsymbol{e}_y$. For incompressible, axisymmetric waves with space-time dependence $\exp(ik_x x + ik_z z - i\omega t)$, the dispersion relation is (Balbus & Hawley 1991)

$$\omega^2 = k_z^2 v_{\mathrm{A}z}^2 + \frac{1}{2}\kappa^2 \frac{k_z^2}{k^2} \pm \frac{1}{2}\left[\left(\kappa \frac{k_z}{k}\right)^4 + 16 k_z^2 v_{\mathrm{A}z}^2 \Omega^2 \frac{k_z^2}{k^2}\right]^{1/2}, \tag{6}$$

where the positive sign gives inertial waves and the negative sign the MRI. Here $v_{\mathrm{A}z} = B_z/(4\pi\rho)^{1/2}$ is the vertical Alfven speed and $\kappa = [2(2-q)]^{1/2}\Omega$ is the fluid epicyclic frequency.[4] In the zero field limit, incompressible inertial waves have the dispersion relation $\omega^2 = \kappa^2 k_z^2/k^2$.

Although inertial modes modified by magnetic tension exist for the constant background chosen above, once the medium becomes turbulent, their possible existence as normal modes of oscillation becomes highly questionable. Low order inertial waves have frequencies of the same order as the energy-bearing MRI "eddies", and hence are susceptible to nonlinear interactions with the MRI turbulence.

The simulations described here have zero net magnetic flux in each direction. Furthermore, the time and space-averaged magnetic pressure is small. We attempt to understand waves in such a turbulent background by again linearizing about a time-independent background with constant density and pressure, velocity $\boldsymbol{v} = -q\Omega x \boldsymbol{e}_y$, but now including compressibility and neglecting magnetic fields. In this case, axisymmetric inertial-acoustic waves satisfy the dispersion relation

$$\omega^2 = \frac{1}{2}\left(\kappa^2 + c_s^2 k^2\right) \pm \frac{1}{2}\left[\left(\kappa^2 + c_s^2 k^2\right)^2 - 4\kappa^2 c_s^2 k_z^2\right]^{1/2}. \tag{7}$$

For zero wavenumber one recovers the fluid epicyclic mode $\omega^2 = \kappa^2$. In the limit $\kappa^2 \ll c_s^2 k^2$, which is a good approximation even for the lowest wavenumbers in our simulations, inertial waves again have the dispersion relation $\omega^2 = \kappa^2 k_z^2/k^2$, while acoustic waves satisfy $\omega^2 = c_s^2 k^2$. In a shearing box of dimensions (L_x, L_y, L_z), these waves will occur at discrete frequencies because the wavenumbers will be quantized according to

$$k_x = \frac{2\pi n_x}{L_x} \quad \text{and} \quad k_z = \frac{2\pi n_z}{L_z}, \tag{8}$$

where n_x and n_z are integers.

Because of the shearing boundary conditions, non-axisymmetric waves in the shearing box have an amplitude and frequency which change with time (Goldreich & Lynden-Bell 1965), and therefore do not exist as normal modes. The radial wavenumber changes with time as $k_x(t) = k_x' + q\Omega(t - t_0)k_y'$, where k_x' and k_y' are the wavenumbers with respect to comoving coordinates $[x, y' = y + q\Omega x(t - t_0)]$, and t_0 is the time of minimum $k_x(t)$. When $k_x(t) \sim k_x'$, non-axisymmetric waves have similar frequencies to axisymmetric waves. For $k_x(t) \gg k_x'$, an approximate WKB dispersion relation for the time-dependent frequency is (see eq. 72 in Goldreich & Lynden-Bell 1965) $\omega(t) \simeq c_s k_y' q\Omega t$, showing that the frequency changes on the shear timescale of the disk. As $k_x(t)$ becomes large, eventually the wave will damp away. If the wave has lifetime T, then we expect it to give rise to a broad peak in the power spectrum of width $\sim c k_y' q\Omega T$ around the corresponding axisymmetric mode.

[4] Not to be confused with the epicyclic frequency of a particle in a gravitational field.

3. POWER SPECTRA

Our simulations use box size $(L_x, L_y, L_z) = (1.25, 4, 1)$ with $(N_x, N_y, N_z) = (40, 64, 32)$ grid points in each direction, respectively. The shear parameter $q = 3/2$, corresponding to Keplerian rotation. The net magnetic flux in each direction is zero and the initial weak field has a spatial dependence given by $\mathbf{B} = B_0 \cos(2\pi x/L_x)\mathbf{e}_y + B_0 \sin(2\pi x/L_x)\mathbf{e}_z$. The initial magnetic pressure is 400 times less than the gas pressure. The sound speed, orbital frequency, and average density have the constant values $c_s = \Omega = 10^{-3}$ and $\rho = 1$. The fiducial simulation is run for 1000 orbits. Averaged over time and the box, the total magnetic pressure in the turbulence that results is 0.65% of the average gas pressure. However, there is significant variance, with small regions of local magnetic pressure reaching 10% of the gas pressure.

Figure 1 shows "position space" power spectra for density, radial velocity, and vertical velocity fluctuations. Three spectra are plotted for each. Data recorded at a specific point (x, y, z) in the box contain fully non-axisymmetric motions. Fluid motions with nodes along the y-direction contain most of the power in MRI turbulence, hence we also record time series for azimuthally averaged data at the same (x, z) and box-averaged data in order to increase signal to noise for oscillatory modes. We interpolated the data to uniform spacing in time, padded the array to a multiple of two, multiplied by the Bartlett window function to reduce spectral leakage (Press et al. 1992), and used a Discrete Fast Fourier Transform to produce the power spectrum. The power spectra are normalized to the root-mean-square of the time series. To produce figure 1 we binned the power into 512 logarithmically spaced frequency bins in the frequency range shown. This has the effect of multiplying the power spectrum by a factor of ω. The frequency $\omega/2\pi$ is expressed in units of inverse orbital time. Arrows show the position of low order acoustic and inertial waves using eq. (7). While all three panels show curves for non-axisymmetric and axisymmetric data, the box-averaged power is only visible in the plot for v_x, appearing as a sharp peak at $\omega = \kappa = \Omega$, the epicyclic frequency. This epicyclic mode has been reported in previous shearing box simulations (Hawley et al. 1995). Numerical damping causes the sharp decline in power at high frequencies. In runs at higher resolution, this dropoff was pushed to higher frequencies, as expected.

The most striking feature in figure 1 is the axisymmetric sound waves, which appear as sharply defined peaks. The power in these peaks approaches the broad continuum due to non-axisymmetric MRI turbulence, and

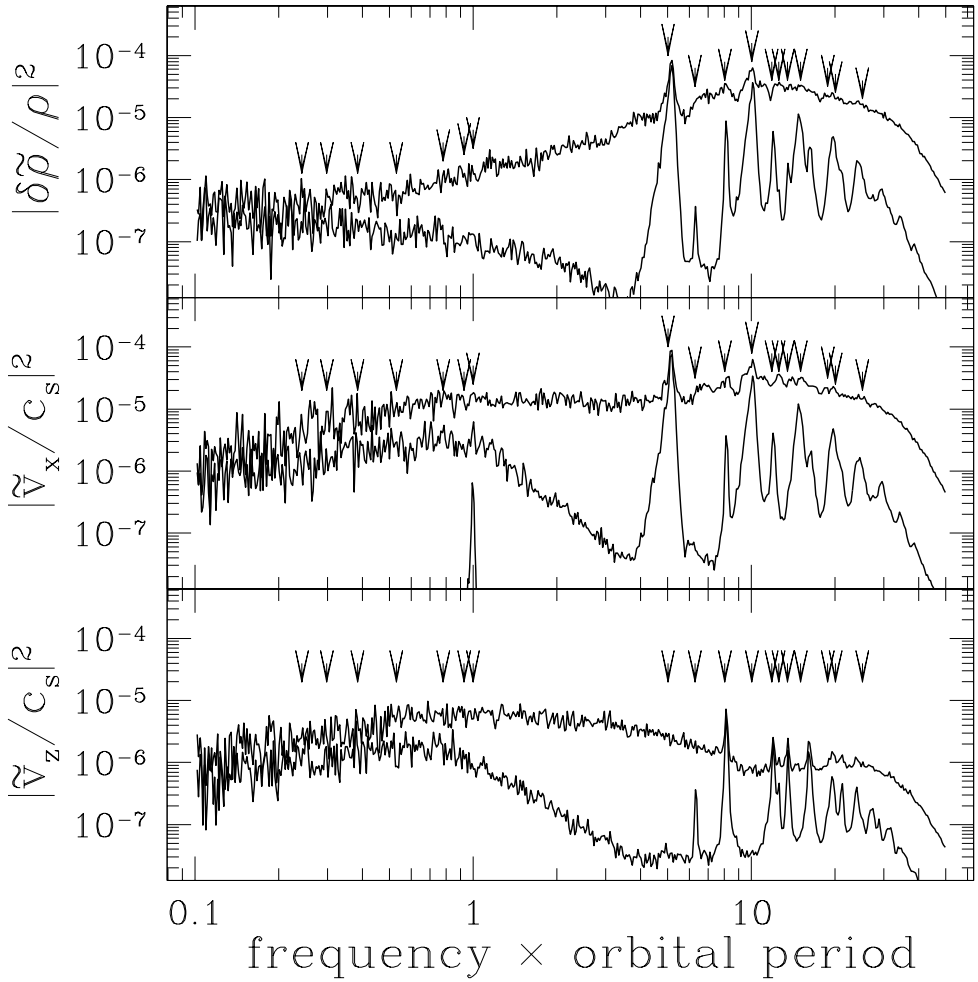

FIG. 1.— "Position space" power spectrum for density (upper), radial velocity (middle), and vertical velocity fluctuations (lower). In each plot, the upper curve is for the non-axisymmetric data and the lower curve is for the axisymmetric data. The sharp peak at the orbital frequency in the middle plot is the box averaged data. The frequency is in units of cycles per orbital period. Power has been rebinned into logarithmically spaced frequency bins, which effectively multiplies the power spectrum by one power of frequency. Axisymmetric hydrodynamic normal mode frequencies from eq. (7) are shown as arrows. The epicyclic mode is at the orbital frequency (unity). Inertial modes and sound waves should lie below and above the epicyclic frequency, respectively. From right to left below the epicyclic frequency, arrows show the expected axisymmetric inertial mode frequencies for $(n_x, n_z) = (1,2), (1,1), (2,1), (3,1), (4,1)$ and $(5,1)$. From left to right above the epicyclic frequency, the axisymmetric acoustic waves have $(n_x, n_z) = (1,0), (0,1), (1,1), (2,0), (2,1), (0,2), (1,2), (3,0), (0,3), (4,0)$, and $(5,0)$, respectively.

clearly rises above the continuum for at least two of the peaks. Axisymmetric sound waves with $n_z = 0$ have much larger density and radial velocity fluctuations than those with $n_x = 0$. This is consistent with the larger continuum seen in v_x relative to v_z. A number of previous investigations (e.g. Stone et al. 1996; Gardiner & Stone 2005) have noted non-axisymmetric sound waves in snapshots of the density profile. These non-axisymmetric sound waves also have $n_z = 0$ and $n_x \neq 0$, consistent with our findings for axisymmetric waves.

There are no significant peaks observed for inertial modes in figure 1. However, this is not proof of their non-existence. The epicyclic mode was buried in the noise for non-axisymmetric and axisymmetric data, and only became visible by box-averaging. Moreover, the *observable* luminosity variation decreases strongly as wavelength decreases, due to averaging of hot and cold spots on the disk. Hence large lengthscale, small power inertial modes may *in principle* be observable as compared to short lengthscale, large power MRI eddies. We now show that this is in fact not the case.

Figure 2 shows the "momentum space" power spectrum. Time series for azimuthally averaged v_x and v_z were computed by taking spatial transforms in the x and z directions, for n_x and n_z nodes, respectively. Hence, turbulent eddies and inertial modes are on the same footing in this plot, as *we compare their power at the same lengthscale*. The temporal power spectrum for the resulting time series was computed as in figure 1 for 128 frequency bins in the range shown. The normalization of the curves is such that the sum over all n_x, n_z, and frequency bins gives the root-mean-square of the time series (compare to axisymmetric curves in figure 1).

The epicyclic mode is again clearly visible in figure 2.

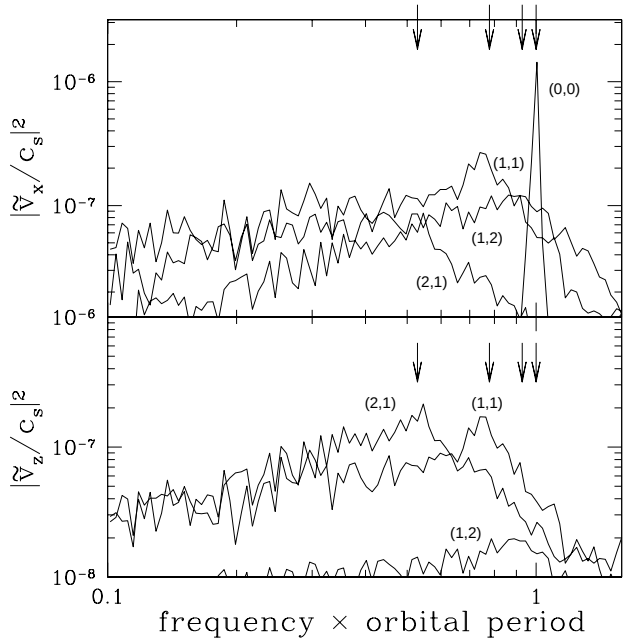

FIG. 2.— "Momentum space" power spectrum for axisymmetric radial velocity (upper), and vertical velocity (lower) fluctuations. Each curve is labelled by (n_x, n_z) used for the spatial Fourier transform. Power has been rebinned into logarithmically spaced frequency bins, which effectively multiplies the power spectrum by one power of frequency. Axisymmetric hydrodynamic inertial mode frequencies from eq. (7) are shown as arrows with $(n_x, n_z) = (0,0), (1,2), (1,1), (2,1)$ from right to left.

The inertial modes are qualitatively different. Two of the lowest order modes show broak peaks of width $\delta\omega \sim \omega$ at the expected frequencies. Without the analytic mode frequencies as a guide, it would be hard to recognize these peaks as significant. Higher order modes (not plotted here) show even less evidence of peaks at the expected frequencies. The lack of clear peaks for inertial modes suggests that they are strongly affected by MRI turbulent stresses. We note that although the epicyclic mode has frequency similar to inertial modes, it is immune to magnetic tension forces as it is nodeless in the shearing box, and hence is less susceptible to turbulent buffeting.

Overall, we find that axisymmetrizing or box-averaging the data from simulations greatly enhances the signal from oscillation modes, a technique easily adapted to global simulations. In addition, long integration times will increase the signal to noise of the nearly sinusoidal waves relative to the stochastic background from turbulence. It is not immediately obvious, however, why we clearly see peaks in our non-axisymmetric data whereas Brandenburg (2005) did not. Perhaps this is because his simulation was stratified in the vertical direction.

4. CONCLUSIONS

We find that turbulence driven by the MRI naturally excites radial epicyclic motion and axisymmetric sound waves, but there is scant evidence of inertial waves. This may imply that inertial modes are strongly affected by MRI turbulent stresses, and cease to exist as high quality oscillators. We note that the zero net magnetic flux simulations presented here give rise to the *weakest* MRI turbulence possible. Inertial waves could be even more strongly affected in simulations with net magnetic flux.

Inertial waves, called "g-modes" in the diskoseismology literature, have been proposed as the origin of some observed QPOs in X-ray binaries (Wagoner 1999; Kato 2001). However, our results imply that all but the longest wavelength of these hydrodynamic modes are destroyed by the turbulence. Even the longest wavelength modes are substantially altered, perhaps to the point of becoming unobservable. This presents a serious problem for models invoking g-modes to explain observed QPOs.

We are not clearly able to pick out non-axisymmetric, shearing waves in the analysis done so far. There are broadened peaks in the non-axisymmetric data around the frequencies of axisymmetric waves, but this is not clear confirmation. Furthermore, "real" accretion disks may in fact admit standing nonaxisymmetric waves with constant pattern speeds. There is substantial global simulation data which demonstrates this fact, at least for hydrodynamic disks (e.g. Blaes & Hawley 1988). The shearing box cannot capture these modes, because the shearing box boundary conditions preclude their existence.

In summary, this paper demonstrates that QPOs can be found in simulations of MRI turbulence, at least in a shearing box geometry. The well-defined boundary conditions of this geometry help ensure the existence of modes, but it is not clear that such well-defined boundaries will exist in real accretion disks. Global MRI simulations could in principle determine self-consistently whether wave cavities exist and contain trapped modes. Traveling acoustic waves have certainly been observed in such simulations (e.g. De Villiers & Hawley 2003), but no evidence for modes at discrete frequencies has yet been reported. We encourage extensions of our analysis techniques to these simulations.

We thank Steve Balbus, Shane Davis, Mike Nowak and Aristotle Socrates for useful discussions. This research was supported by the National Science Foundation under grant nos. PHY99-07949 and AST 03-07657.

REFERENCES

Balbus, S. A., & Hawley, J. F. 1991, ApJ, 376, 214
Blaes, O. M., & Hawley, J. F. 1988, ApJ, 326, 277
Blaes, O. M., Arras, P., & Fragile, C., MNRAS, submitted
Brandenburg, A. 2005, Astronomische Nachrichten, 326, 787
De Villiers, J.-P., & Hawley, J. F. 2003, ApJ, 592, 1060
Gardiner, T. A., & Stone, J. M. 2005, in Magnetic Fields in the Universe, AIP Conf. Proc., 784, 475
Giannios, D., & Spruit, H. C. 2004, A&A, 427, 251
Goldreich, P., & Lynden-Bell, D. 1965, MNRAS, 130, 125
Hawley, J. F., Gammie, C. F., & Balbus, S. A. 1995, ApJ, 440, 742
Kato, S. 2001, PASJ, 53, 1
Kluźniak, W., Abramowicz, M. A., Kato, S., Lee, W. H., & Stergioulas, N. 2004, ApJ, 603, L89
Lee, W. H., Abramowicz, M. A., & Kluźniak, W. 2004, ApJ, 603, L93
McClintock, J. E., & Remillard, R. A. 2004, in Black Hole Binaries, eds. W. H. G. Lewin & M. van der Klis (Cambridge: Cambridge Univ. Press), in press

Nowak, M. A., & Wagoner, R. V. 1993, ApJ, 418, 187
Nowak, M. A., & Wagoner, R. V. 1995, MNRAS, 274, 37
Press, W. H., Teukolsky, S. A., Vetterling, W. T., & Flannery, B. P. 1992, (Cambridge: Cambridge Univ. Press)
Rezzolla, L., Yoshida, S., Maccarone, T. J., & Zanotti, O. 2003, MNRAS, 344, L37
Stone, J. M., Hawley, J. F., Gammie, C. F., & Balbus, S. A. 1996, ApJ, 463, 656
van der Klis, M. 2004, in Black Hole Binaries, eds. W. H. G. Lewin & M. van der Klis (Cambridge: Cambridge Univ. Press), in press
Wagoner, R. V. 1999, Phys. Rep., 311, 259